ISSN (Print) 1226-1750
ISSN (Online) 2233-6656
Journal of Magnetics 28(4), 339-346 (2023) https://doi.org/10.4283/JMAG.2023.28.4.339

Room-Temperature Exchange Bias and Training Effect in $Co/IrMn_3$ Thin Films with Varying Co Layer Thicknesses

Sunghyuk Song, Yongsub Kim, and Sang-Koog Kim*

National Creative Research Initiative Center for Spin Dynamics and Spin-Wave Devices, Nanospinics Laboratory, Research Institute of Advanced Materials, Department of Materials Science and Engineering, Seoul National University, Seoul 08826, Republic of Korea

(Received 12 July 2023, Received in final form 22 November 2023, Accepted 29 November 2023)

We investigated room-temperature exchange bias phenomenon and training effect in SiO_2/Ru(40 nm)/Co(t nm)/$IrMn_3$(5 nm)/Ta(5 nm) with varying Co layer thicknesses t = 2, 3, 5, 8, 10, and 20 nm. Consecutive hysteresis loop measurements by longitudinal magneto-optical Kerr effect (L-MOKE) revealed the presence of both athermal and thermal training effects in the $Co/IrMn_3$ ferromagnetic/antiferromagnetic bilayers. The athermal training effect is more prominent as the Co layer thickness increased. We also observed that the training effect constant γ increased with increasing Co layer thickness, suggesting that thicker samples were closer to equilibrium, as interpreted by Binek's relaxation model. This study not only advances our understanding of the exchange bias phenomenon and training effect in the $Co/IrMn_3$ system but also may offer their potential for use in neuromorphic devices.

Keywords : exchange bias, training effect, interfacial magnetism, $Co/IrMn_3$

1. Introduction

The manipulation of magnetization configurations and control of related magnetic properties in multilayered thin films have emerged as vital areas of research due to their potential applications in a variety of magnetic and spintronic devices. Among these, the exchange bias phenomenon, first reported in 1956 [1], has attracted significant attention for its capacity to stabilize and shift magnetic hysteresis loops, thereby enabling the control of magnetization configuration and relevant properties such as magnetization and coercive field, as well as exchange bias field. This phenomenon arises from interfacial magnetization states between ferromagnetic (FM) and antiferromagnetic (AFM) materials and has been extensively investigated and applied in numerous applications, such as magnetic sensors, magnetic random access memory (MRAM), and spin valves [2-8].

The training effect, an intriguing aspect of the exchange bias phenomenon, involves changes in the exchange bias field and coercivity with consecutive magnetic hysteresis loop measurements. This effect has been observed in various FM/AFM systems and is considered critical for understanding the underlying mechanisms of exchange bias [9, 10]. Moreover, the training effect holds considerable promise for applications in neuromorphic devices, where multiple magnetization states are essential for efficient information storage and processing devices.

In this study, we investigated room-temperature exchange bias phenomenon and training effect in $Co/IrMn_3$ thin films, as measured by longitudinal magneto-optical Kerr effect (L-MOKE). We focus on the impact of the ferromagnetic Co layer thickness on the exchange bias field, coercivity, and the training effect constant of Binek's relaxation model [11]. Our findings revealed the presence of both athermal and thermal training effects in the $Co/IrMn_3$ FM/AFM system for different Co thicknesses, and we interpreted the results according to Binek's relaxation model. This training effect can potentially be utilized in applications for neuromorphic devices.

This paper is structured as follows: Section 2 describes the sample preparation and experimental methods employed. Section 3 presents the results and discussions, encompassing the exchange bias behavior, training effect observations, and their association with the Co layer

*Corresponding author: Tel: +82-2-880-5854
Fax: +82-2-880-1457, e-mail: sangkoog@snu.ac.kr

thickness. Finally, Section 4 summarizes the conclusions and potential applications derived from our findings.

2. Experimental Procedures

2.1. Sample preparation

There are two main methods to fabricate specimens exhibiting exchange bias. The first method involves the magnetic field cooling technique where annealing of samples up to Néel temperure is necessary, and the second method is the field deposition method, where the fabrication of layered films is done simultaneously under applying a sufficiently strong magnetic field. To minimize the formation of intermixing layers at the interface between the ferromagnetic (FM) and antiferromagnetic (AFM) layers through diffusion during annealing [12], we fabricated samples using the field deposition method. To fabricate the specimens using this method, a holder with 0.3 kOe strength magnets attached to both sides was used. The substrate was placed between the magnets, the top part of the holder was assembled to secure the substrate, and deposition was carried out using DC magnetron sputtering. All deposition processes were conducted under ultra-high vacuum conditions, maintaining a pressure below 10^{-9} Torr. The $IrMn_3$ AFM layer was deposited using a target with an atomic composition of 22:78, as shown in Table 1.

Our samples' structure is the top-pinned structure, as shown in Fig. 1, where a Co FM layer was deposited directly onto a Ru seed layer, followed by the deposition of an $IrMn_3$ AFM layer, and then a Ta capping layer was deposited. In this layer arrangement, the AFM layer is 'pinned' as the top of the structure, with the FM layer situated beneath it. During the layered films deposition, a 0.3 kOe magnetic field was applied.

In more detail, an hcp (002) Ru was employed as a seed layer [13]. Previous research has demonstrated that a 40 nm thickness of the Ru layer yields the largest exchange bias field, so we opted for this thickness in our deposition process. It has been reported that the training effect is primarily observed for AFM layer thicknesses ranging between 3 nm and 10 nm. However, for thicker AFM layers, the exchange bias is well-established, while the training effect is less prominent. Therefore, we selected a 5 nm thickness for the $IrMn_3$ AFM layer in our samples based on the findings from previous studies [14-18]. In the case of the FM layer, smaller thicknesses below a certain critical value result in a significant reduction in exchange bias. To circumvent this issue, our samples were fabricated with a minimum thickness of 2 nm for Co, in accordance with the findings reported in the literature [19], and we varied the Co layer thickness as t = 2, 3, 5, 8, 10, and 20 nm in the given structure shown in Fig. 1, to examine the training effect as a function of Co thickness.

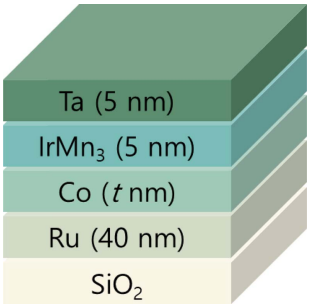

Fig. 1. (Color online) Sample layered structure of Ru(40 nm)/Co(t nm)/IrMn3(5 nm)/Ta (5 nm) for top pinned layer, where the Co thickness t varies as t = 2, 3, 5, 8, 10, and 20 nm.

2.2. Hysteresis loop measurements

To measure consecutive magnetization hysteresis loops of exchange bias films, a custom-built L-MOKE instrument was employed, as illustrated in Fig. 2. In the measurement geometry, the plane of light incidence, containing both the incident and reflected light, is parallel to the sample's magnetization orientation. By monitoring changes in the polarization and intensity of the incident light as a laser irradiates the surface of a magnetized sample, the in-plane magnetization components can be effectively measured in exchange-bias thin-film samples. To investigate the training effect, we performed hysteresis loop measurements in a range between $H = -1.0$ and 1.0 kOe at a step of 0.01 kOe for up to 20 iterations, with

Table 1. Deposition conditions for each layer using DC magnetron sputtering.

Layer	Composition	Base Pressure [Torr]	Working Pressure [mTorr]	Deposition rate [Å/s]
Ru		$<10^{-9}$	1	1.534
Co		$<10^{-9}$	1	0.397
$IrMn_3$	22:78	$<10^{-9}$	1	1.437
Ta		$<10^{-9}$	3	0.832

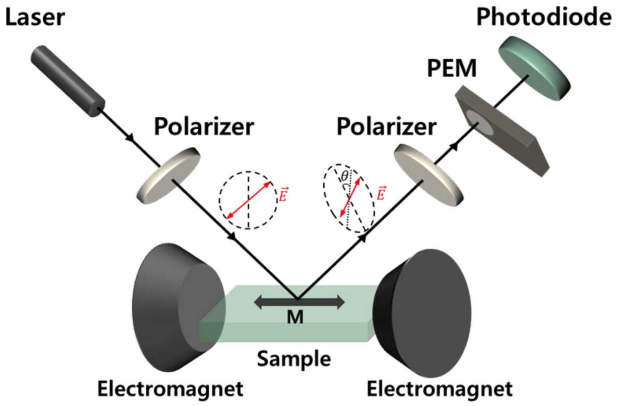

Fig. 2. (Color online) Schematic representation of a Longitudinal Magneto-Optic Kerr Effect (L-MOKE) setup.

each complete loop measurement.

3. Results and Discussion

3.1. Structural characterization

The crystal structure of each layer within layered thin films is known to be influenced by the underlying layer in exchange bias samples. Specifically, for $IrMn_3$ as an AFM layer, the $L1_2$ (111) phase is necessary for the occurrence of exchange bias [20]. To investigate the crystal structure of the fabricated samples, X-ray diffraction (XRD) measurements were performed. When using a Ru seed layer, the field cooling method would enhance the intensity of the $IrMn_3$ fcc (111) peak. However, in our case for samples fabricated with the field deposition method, the intensity of the $IrMn_3$ fcc (111) peak is relatively low and difficult to distinguish it from the Ru hcp (002) peak, as shown in Fig. 3. Indeed, the interference of the $IrMn_3$ and Co peaks with Ru peaks rendered it impossible to confirm the difference in peak intensity between the Co and $IrMn_3$ layers for various Co thicknesses (see Fig. 3). Nevertheless, previous studies have reported that, for the top-pinned structure sample employed in this experiment, this factor does not significantly influence the magnitude of the exchange bias field among the various factors affecting it [15].

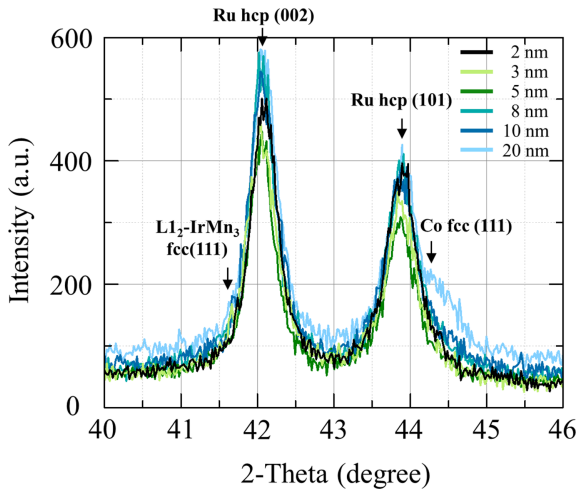

Fig. 3. (Color online) XRD patterns of layered films of Ru(40 nm)/Co(t nm)/IrMn3(5 nm)/Ta (5 nm) samples with different Co thicknesses, t = 2, 3, 5, 8, 10, and 20 nm.

3.2. Exchange bias and training effect

For the samples we fabricated, we measured the first cycle of hysteresis loop for various Co thicknesses using the aforementioned L-MOKE technique. Among the samples, the one with $t = 2$ nm exhibited the largest exchange bias field $H_{EB} = 275$ Oe and coercivity $H_C = 177$ Oe. As t increased further, H_{EB} gradually decreased to $H_{EB} = 6$ Oe for $t = 20$ nm, while H_C decreased up to $H_C = 95$ Oe for $t = 20$ nm, as illustrated in Fig. 4. The plots of H_{EB} and H_C versus t are given in Fig. 5. It is evident that the decrease of H_C becomes slower from 5 nm to 20 nm, while H_{EB} decreases relatively significantly until t = 20 nm.

Subsequently, to investigate the tendency of training effects for different t values, we conducted additional cycles of hysteresis loop measurements, with n = 1, 2, 3, 5, 10, and 20, where n represents the cycle number of hysteresis loop measurements. Generally, for all t values, the coercivities of left (H_{C1}) and right (H_{C2}) sides exhibit a shift towards a decrease (toward $H = 0$).

The measured hysteresis loops for each Co thickness at n = 1, 2, 3, 5, 10, and 20 measurement cycles were shown in Fig. 6. For $t = 2$ nm, H_{C1} and H_{C2} shift to the right by 71 Oe and 50 Oe, respectively. For all the samples, the coercivity H_{C1} and H_{C2} both shift to the right with increasing cycling, n; however, for thicker Co layers the training effect becomes weaker. This demonstrates that the Co/$IrMn_3$ bilayer system exhibits a distinct training effect, which varies with different Co layer thicknesses. In Fig. 7, we plotted H_{EB} and $H_{EB}(n)$–$H_{EB}(n=1)$ versus n to investigate athermal and thermal training effects for the different Co thicknesses. As the Co thickness increases, the exchange bias is reduced more significantly with increasing n.

In fact, it is known that the athermal training effect and thermal training effect are two distinct mechanism that describe how the exchange bias field changes with consecutive hysteresis loop measurements. The athermal training effect refers to the significant change in the exchange bias field that occurs between the first and

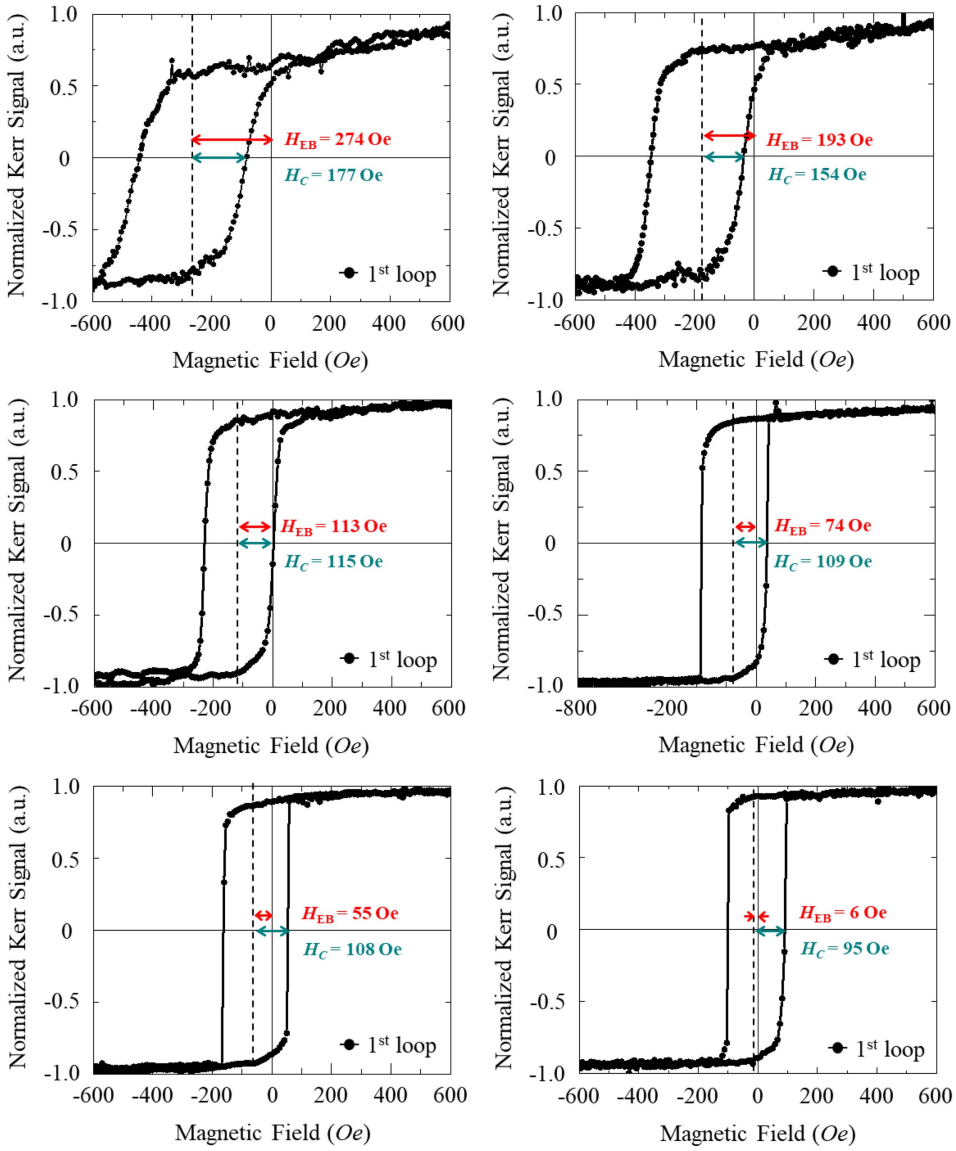

Fig. 4. (Color online) First cycling of magnetization hysteresis loops measured by L-MOKE for individual exchange biased samples with (a) t = 2 nm, (b) t = 3 nm, (c) t = 5 nm, (d) t = 8 nm, (e) t = 10 nm, (f) t = 20 nm.

second hysteresis loops. This effect is characterized by a rapid decrease in the exchange bias field during the initial cycling, and it is not directly related to temperature. The athermal training effect is typically attributed to the realignment or reorganization of magnetic moments at the FM/AFM interface during the initial magnetization cycling.

In contrast, the thermal training effect refers to the gradual change in the exchange bias field that occurs after the second hysteresis loop measurement as the system approaches equilibrium. This effect is more sensitive to temperature, and it results from the progressive relaxation of magnetic moments in the AFM layer as the magnetization cycling continues. The thermal training effect generally exhibits a slower rate of change in the exchange bias field compared to the athermal training effect. Thus, we need to interpret the observed reduction of H_{EB} with increasing n for different Co thicknesses.

3.3. Binek's relaxation model

The training effect unveils a gradual decline in exchange bias and coercivity as the cycling number (n) increases. Diverse endeavors have been dedicated to elucidating this phenomenon through a power law. Nevertheless, the sudden alterations arising from athermal effect between n = 2 and n = 1 resist characterization within the confines of a power-law framework. Thus, where the most pronounced reduction in the exchange bias field occurred between the first and second hysteresis loops,

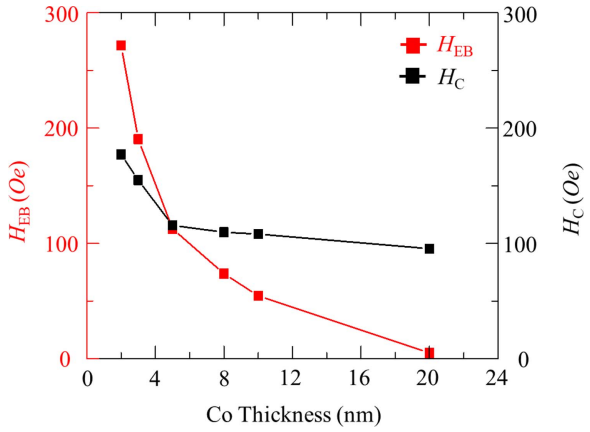

Fig. 5. (Color online) Exchange bias field (H_{EB}) and coercivity (H_C) as a function of Co layer thickness were obtained from the first cycle of hysteresis loop measurement.

the power law cannot explain our results. In this case, the power law can be fitted starting from $n = 2$ to obtain the equilibrium exchange bias field, H_{BB}^{e}. However, Binek's relaxation model successfully elucidates the training effect from $n = 1$ onwards. Considering each state for cycling number (n) as a metastable state and accounting for spin configuration relaxation, the system undergoes a relaxation process towards equilibrium as n increases. This relaxation process towards equilibrium can be represented by the discretized Landau-Khalatnikov equation, resulting in Binek's equation

$$\mu_0[H_{EB}(n+1) - H_{EB}(n)] = -\gamma\{\mu_0[H_{EB}(n) - H_{EB}^{e}]\}^3 \quad (1)$$

where γ is the training effect constant, serving as an

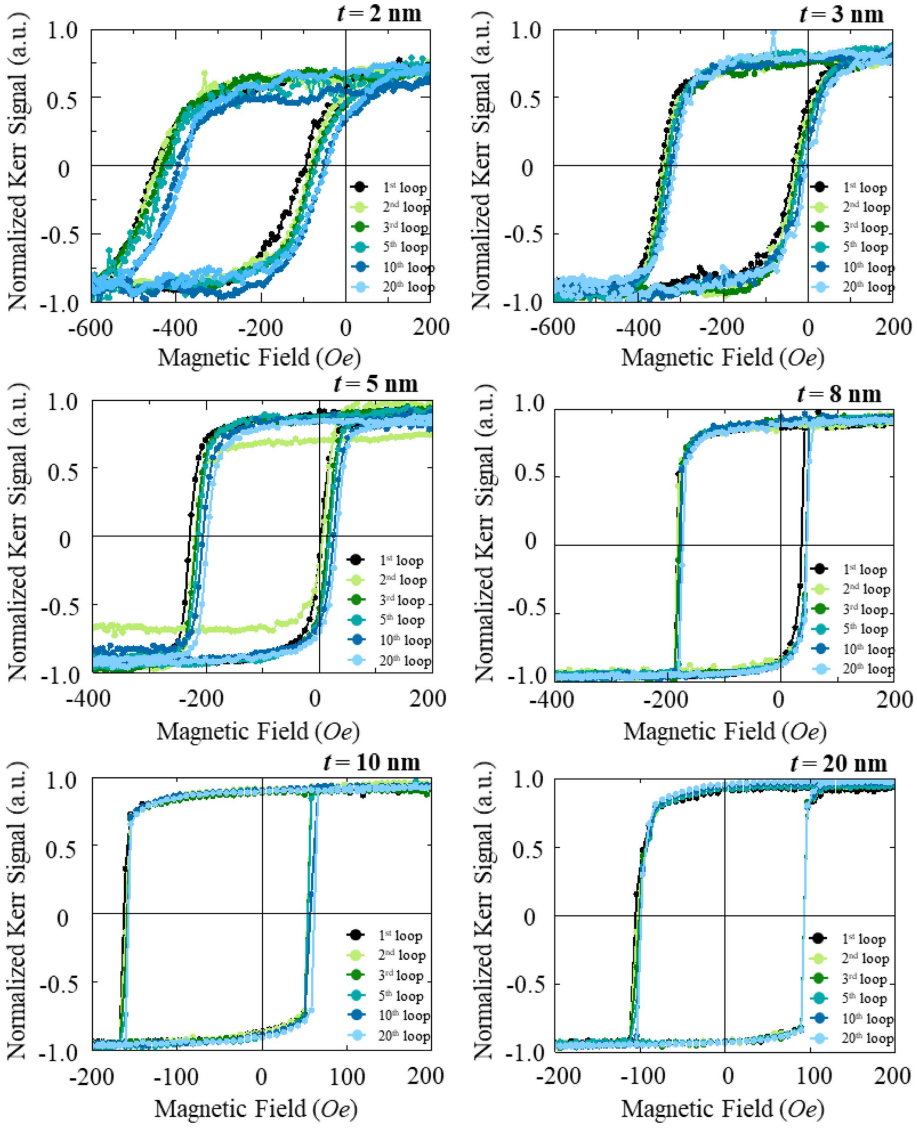

Fig. 6. (Color online) Consecutive hysteresis loop measurement with cycling number n = 1, 2, 3, 5, 10, and 20 for different Co thicknesses; (a) t = 2 nm, (b) t = 3 nm, (c) t = 5 nm, (d) t = 8 nm, (e) t = 10 nm, (f) t = 20 nm.

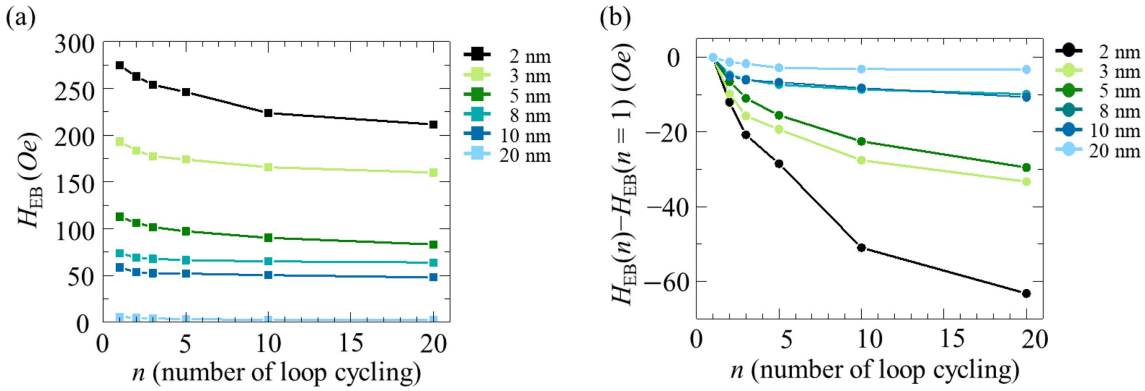

Fig. 7. (Color online) (a) Exchange bias field as a function of the number n of hysteresis loop measurement cycling, (b) $H_{EB}(n)-H_{EB}(n=1)$ as a function of n for various t values.

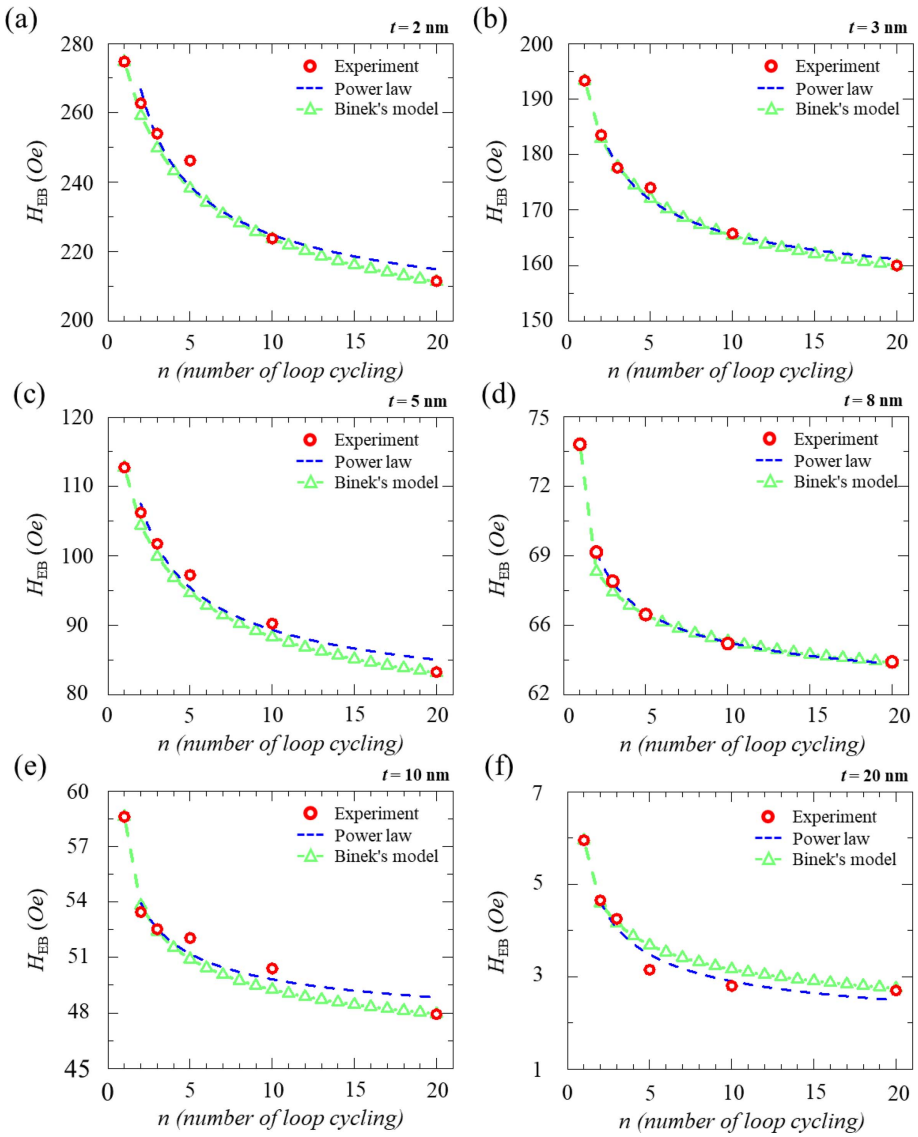

Fig. 8. (Color online) Fitting results using a Power law (blue dashed lines) from n = 2 to n = 20, and Binek's relaxation model (green triangle-dotted line) for n = 1 to n = 20 for (a) t = 2 nm, (b) t = 3 nm, (c) t = 5 nm, (d) t = 8 nm, (e) t = 10 nm, (f) t = 20 nm.

Table 2. Equilibrium exchange bias field (H_{EB}^{e}), power-law fitting parameter and training effect constant (γ) for Ru(40 nm)/Co(t nm)/$IrMn_3$(5 nm)/Ta(5 nm) layered samples with varying Co layer thicknesses (t). (power-law: $H_{EB}(n) = H_{EB}^{e} + \frac{\kappa}{\sqrt{n}}$)

Co thickness	2 nm	3 nm	5 nm	8 nm	10 nm	20 nm
H_{EB}^{e} (Oe)	190.9 ± 20.1	150.5 ± 6.0	74.7 ± 6.9	62.1 ± 0.3	46.5 ± 3.4	1.5 ± 1.0
κ	107.3 ± 43.4	47.7 ± 12.3	46.4 ± 14.2	9.92 ± 0.6	10.51 ± 6.9	4.4 ± 2.1
γ	1.2×10^{-5}	9.0×10^{-5}	9.3×10^{-5}	3.2×10^{-3}	1.6×10^{-3}	1.7×10^{-2}

indicator of the system's response to consecutive hysteresis loop measurements and the rate at which it approaches equilibrium. H_{EB}^{e} represents the exchange bias field in the limit of infinite loops [11].

A larger value of γ implies a smaller absolute magnitude of the training effect and a state that is closer to equilibrium. We present the fitting results for plots of H_{EB} versus n using Eq. (1) (see Fig. 8). The fitting result (green triangle-dashed line) from n = 1 to n = 20 using Eq. (1) provides a better representation of the observed behavior compared to the fitting results from n = 2 to 20 using a power law (blue dashed lines). This demonstrates that the model employed in Eq. (1) is more appropriate for describing the training effect in our Co/$IrMn_3$ system.

Upon evaluating H_{EB}^{e} and γ for each sample, it becomes evident that γ increases with the growth of the Co layer thickness. While the γ for t = 10 nm appears to decrease, it is likely attributable to experimental error. Across the entire sample, there was an observed tendency of increasing γ and decreasing H_{EB}^{e} with respect to t. This observation corroborates that the state approaches equilibrium as the Co layer thickness increases (see Table 2).

Our experimental results up to n = 20 indicate that the specific magnetization states in both the AFM and FM layers, as well as their interface at n = 20, have not yet reached their equilibrium states, achieving the equilibrium exchange bias field (H_{EB}^{e}). We can anticipate that further measurements (n = 21, 22, ...) will eventually lead to the equilibrium state and its corresponding value of H_{EB}^{e}.

Nonetheless, from a technological perspective and for practical applications, such metastable magnetization states (e.g., varying H_C values with n) can offer 20 distinct multistates at room temperature. This feature could provide a considerable advantage for the implementation of multistate and stochastic neuromorphic devices.

4. Summary

We investigated the room-temperature exchange bias phenomenon and training effect in Co/$IrMn_3$ FM/AFM bilayer thin films with varying Co thicknesses. As the number of consecutive hysteresis loop measurements increased, the exchange bias field decreased, resulting in the training effect. The most substantial decrease in exchange bias occurred between the first and second hysteresis loop measurements, revealing the athermal training effect. As the FM Co layer thickness increased, both the exchange bias field and the coercivity decreased, demonstrating that the athermal training effect was more prominent as the Co thickness increased during the process. The athermal training effect was observed in samples with thicker Co layers, while the normal thermal training effect was dominant in thinner Co layers. According to Binek's relaxation model, the training effect constant γ also increased with the Co thickness, verifying that the thicker samples were closer to equilibrium.

Since the samples of this structure have not yet reached the equilibrium states, *i.e.* the equilibrium exchange bias field (H_{EB}^{e}) at n = 20, it is expected that the exchange bias field will exhibit additional training effects until it reaches equilibrium (H_{EB}^{e}) when conducting more than 20 measurements (n = 21, 22, ...). From an application perspective, the fact that the sample of this structure has more than 20 states at room temperature holds significant potential for its use in neuromorphic devices.

Acknowledgements

This research was supported by the Basic Science Research Program through the National Research Foundation of Korea (NRF) funded by the Ministry of Science, ICT, and Future Planning (No. NRF-2021R1A2C2013543). The Institute of Engineering Research at Seoul National University provided additional research facilities for this work.

References

[1] W. H. Meiklejohn *et al.*, Phys. Rev. **102**, 1413 (1956).
[2] J. Nogués *et al.*, J. Magn. Magn. Mater. **192**, 203 (1999).
[3] J. C. S. Kools, IEEE Trans. Magn. **32**, 3165 (1996).
[4] A. V. Khvalkovskiy *et al.*, J. Phys. D: Appl. Phys. **46**,

074001 (2013).
[3] C. Tsang *et al.*, IEEE Trans. Magn. **30**, 3801 (1994).
[5] D. Paccard *et al*., Phys. Status. Solidi B **16**, 301 (1966).
[6] D. Suess *et al.*, Phys. Rev. B **67**, 054419 (2003).
[7] F. Dorfbauer *et al.*, J. Magn. Magn. Mater. **290**, 754 (2005).
[8] A. Hoffmann, Phys. Rev. Lett. **93**, 097203 (2004).
[9] T. Hauet *et al.* Phys. Rev. Lett. **96**, 067207 (2006).
[10] A. Biternas Ph.D Dissertaion, University of York (2009).
[11] C. Binek, Phys. Rev. B **70**, 014421 (2004).
[12] K.-S. Lee *et al.*, Appl. Phys. Lett. **86**, 192512 (2005).
[13] M. Pakala *et al.*, J. Appl. Phys. **87**, 6653 (2000).
[14] H. Xi *et al.*, Phys. Rev. B **64**, 184416 (2001).
[15] K. Zhang *et al.*, J. Appl. Phys. **91**, 6902 (2002)).
[16] I. Dzhun *et al.*, Acta Phys. Pol. A **127**, 555 (2015).
[17] V. Rodionova *et al*., Solid State Phenomena. Vol. 233. Trans Tech Publications (2015).
[18] C. Gritsenko *et al.*, Phys. Procedia **82**, 51 (2016).
[19] D. Mauri *et al.*, J. Appl. Phys. **62**, 2929 (1987).
[20] A. Kohn *et al*., Sci. Rep. **3**, 2412 (2013).